

# TGA-MS Studies of the Pyrolysis of Corn Stover for Charcoal Production

by

Tachmajal Marie Corrales Sanchez

Submitted to the Department of Mechanical Engineering  
in partial fulfillment of the requirements for the degree of

Bachelor of Science in Mechanical Engineering

at the

MASSACHUSETTS INSTITUTE OF TECHNOLOGY

February 2016

© Massachusetts Institute of Technology 2016. All rights reserved.

Signature redacted

Author .....

Department of Mechanical Engineering

December 28, 2015

Signature redacted

Certified by .....

Gwyndaf Jones

Research Technical Specialist

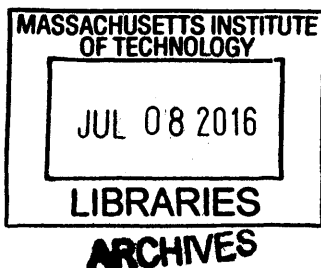
Thesis Supervisor

Signature redacted

Accepted by .....

Anette Hosoi

Associate Professor of Mechanical Engineering





# TGA-MS Studies of the Pyrolysis of Corn Stover for Charcoal Production

by

Tachmajal Marie Corrales Sanchez

Submitted to the Department of Mechanical Engineering  
on December 28, 2015, in partial fulfillment of the  
requirements for the degree of  
Bachelor of Science in Mechanical Engineering

## Abstract

More than two billion people worldwide rely on wood-based fuels for their daily energy needs, which can produce toxic atmospheric contaminants and cause environmental degradation. MIT D-Lab addresses this challenge with "Fuel from the Fields", a simple technique for making charcoal from agricultural waste. In this work, Thermo-gravimetric analysis combined with online mass spectrometry (TGA-MS) was used to study the pyrolysis of corn agricultural waste with the aim of improving understanding of the carbonization process. Non-isothermal mass loss data from TGA was obtained for three types of corn waste, cobs, husks, and stalks; and used to calculate proximate analysis in terms of moisture, volatile matter, and charcoal content. TGA-MS data for the three materials was used to understand the emissions of  $H_2O$ ,  $CO$ ,  $H_2S$  and  $C_4H_2$  as a function of temperature. Activation energy,  $E_a$ , and pre-exponential factor,  $A$ , were calculated using the first order global single reaction model for corn cobs and husks. TG-DTG data suggested that corn cobs are better suited feedstocks for charcoal production. Mass Spectroscopy was found to successfully characterize emissions. For corn cobs,  $A = 1.3 \cdot 10^5 s^{-1}$  and  $E_a = 88.6 kJ/mol$ , while for husks  $A = 5.2 \cdot 10^5 s^{-1}$  and  $E_a = 96.4 kJ/mol$ . Based on this work, a carbonization burn timeline worksheet was created to aid monitoring of char yield in the field.

Thesis Supervisor: Gwyndaf Jones  
Title: Research Technical Specialist



## Acknowledgments

I would like to express my sincere gratitude to my advisor Gwyndaf Jones and my supervisor Daniel Sweeney. Your support, patience, knowledge and motivation made this work possible.

I would also like to thank Nancy Adams, Jack Whipple, Becca Smith, Amy Smith, Victor Grau Serrat, Kofi Taha, and the D-Lab family, for giving me the opportunity of being part of D-Lab and thanks to whom I was able to participate of many life-changing experiences.

I would like to thank my friends Ariana, Jenny, Andrea, Varun, Al, Raul, Majo, and Rafael. Your encouragement and support was invaluable to me.

Last but not least, I would like to thank my family: my mother Rut, my grandmother Marta, my grandfather Toni, my brother Camelot, and my sister Darat. You are my source of inspiration, and without your unconditional support, none of this would have been possible.



# Contents

<b>1</b>	<b>Introduction</b>	<b>17</b>
1.1	Household Fuel Combustion . . . . .	17
1.2	Charcoal as an Alternative Fuel for Less-Resourced Settings . . . . .	19
1.2.1	Wood-fuels Usage . . . . .	19
1.2.2	Charcoal from Agricultural Residues . . . . .	19
1.2.3	Fuel from the Fields: MIT D-Lab's Work . . . . .	20
<b>2</b>	<b>Experimental Design</b>	<b>23</b>
2.1	Biomass Composition . . . . .	23
2.1.1	Ligno-cellulosic Composition of Herbaceous Biomass . . . . .	23
2.1.2	Proximate Analysis . . . . .	24
2.2	Pyrolysis and Thermal Analysis . . . . .	24
2.2.1	Overview of Pyrolysis and Decomposition Kinetics . . . . .	24
2.2.2	Thermogravimetric Analysis . . . . .	26
2.3	Materials and Methods . . . . .	28
2.3.1	Strategy . . . . .	28
2.3.2	Material Preparation . . . . .	29
2.3.3	Experimental Set-up . . . . .	30
<b>3</b>	<b>Results and Discussion</b>	<b>33</b>
3.1	TG-DTG Curves . . . . .	33
3.1.1	Corn Cobs . . . . .	34
3.1.2	Corn Husks . . . . .	36

3.1.3	Corn Stalks . . . . .	38
3.1.4	Comparisons Between Experiments 1 and 2 . . . . .	39
3.2	Proximate Analysis and Char Yield . . . . .	40
3.3	Emissions from Mass Spectroscopy . . . . .	41
3.4	Effect of Heating Rate . . . . .	44
3.5	Determination of $E_a$ and $A$ . . . . .	45
3.6	Other Considerations . . . . .	47
<b>4</b>	<b>Worksheet for Char Yield Monitoring</b>	<b>49</b>
<b>5</b>	<b>Conclusion</b>	<b>53</b>
<b>A</b>	<b>MATLAB Code</b>	<b>55</b>
A.1	TGA-DTGA Data Analysis . . . . .	55
A.2	$E_a$ calculation . . . . .	56
A.3	$A$ calculation . . . . .	58



# List of Figures

1-1	MIT D-Lab Charcoal Process Methodology . . . . .	22
2-1	Stages of biomass pyrolysis in a TG-DTG curve . . . . .	27
2-2	Corn stover samples and mill . . . . .	29
2-3	TGA-MS Experimental Set-up . . . . .	30
3-1	TG-DTG curve for corn cob sample C-1 with heating rate 20 °C/min	34
3-2	TG-DTG curve for corn cob sample C-2 with heating rate 2 °C/min .	35
3-3	TG-DTG curve for corn cob sample C-3 with heating rate 10 °C/min	35
3-4	TG-DTG curve for corn husk sample H-1 with heating rate 20 °C/min	36
3-5	TG-DTG curve for corn husk sample H-2 with heating rate 2 °C/min	37
3-6	TG-DTG curve for corn husk sample H-3 with heating rate 10 °C/min	37
3-7	TG-DTG curve for corn stalk sample S-1 with heating rate 20 °C/min	38
3-8	TG-DTG curve for corn stalk sample S-2 with heating rate 2 °C/min	38
3-9	TG and DTG curves for Experiments 1 and 2. . . . .	39
3-10	Abundance as a function of TGA temperature profile for $m/z = 18$ .	42
3-11	Abundance as a function of TGA temperature profile for $m/z = 28$ .	42
3-12	Abundance as a function of TGA temperature profile for $m/z = 34$ .	43
3-13	Abundance as a function of TGA temperature profile for $m/z = 50$ .	43
3-14	TG and DTG curves for Experiments 2 and 3. . . . .	44
3-15	Logarithm of heating rate vs. reciprocal absolute temperature for equivalent mass percentage losses of cob samples at 2 °C/min and 10 °C/min . . . . .	45

3-16	Logarithm of heating rate vs. reciprocal absolute temperature for equivalent mass percentage losses of husk samples at 2 °C/min and 10 °C/min . . . . .	46
4-1	Charcoal burn worksheet page 1. . . . .	50
4-2	Charcoal burn worksheet page 2. . . . .	51

# List of Tables

2.1	Detail of samples and experiments performed . . . . .	31
3.1	Proximate analysis for corn stover samples from TGA data . . . . .	41
3.2	Kinetic parameters obtained for corn cobs and husks pyrolysis . . . . .	46



# Terminology

**Activation Energy ( $E_a$ ).** Minimum energy needed to drive a chemical reaction.

**Arrhenius Equation.** Describes reaction rates of a chemical reaction as a function of the pre-exponential constant  $A$ , activation energy  $E_a$ , universal gas constant  $R$ , and temperature  $T$ .

**Ash.** Solid inorganic residues after carbonization.

**Carbonization.** Conversion of biomass to char through pyrolysis.

**Char.** Solid materials composed of carbon and ash remaining after carbonization.

**Char Yield ( $C.Y.$ ).** Ratio expressed as percentage between the amount of initial material that underwent carbonization and the amount of final material remaining after conversion has finalized, which includes ash and carbon.

**Charcoal.** Solid fuel produced by carbonization of biomass after post-processing.

**Cellulose.** Long and crystalline polymer of formula  $(C_6H_{10}O_5)_n$  that is one of the principal components of herbaceous biomass and provides structural support.

**Corn Cobs.** Corn agricultural residue that refers to the corn cob and includes the hard wood ring, soft center pith, and outer soft beeswing, but does not include

kernels or shank.

**Corn Husks.** Corn herbaceous matters that surrounds the cob, not including the shank. Also known as bracts.

**Corn Stalks.** Corn vascular tissue (stem) that grows above the ground without including leaves.

**Corn Stover.** All parts of the corn plant that grow above the ground, not including the grain.

**Heating Rate.** Rate of temperature increase per unit time.

**Hemicellulose.** Amorphous polymer of formula  $(C_5H_8O_4)_m$  that is one of the principal components of herbaceous biomass.

**Lignin.** Complex, highly branched polymer that is one of the major components of herbaceous biomass.

**Ligno-cellulosic materials.** Non-starch, fibrous components of herbaceous plants composed primarily of cellulose, hemicellulose and lignin.

**Mass Spectroscopy (MS).** Analytical technique used to identify the chemical nature of a sample by measuring the mass-to-charge ratio ( $m/z$ ) and abundance of its gaseous ionized fragments.

**Pre-exponential factor ( $A$ ).** Pre-exponential constant of the Arrhenius equation, determined experimentally, that relates to the frequency at which molecular collisions occur in a substance.

**Pyrolysis.** Thermochemical decomposition of biomass at high temperatures in an inert gaseous atmosphere.

**Rate constant ( $k$ ).** Constant that describes the kinetic reaction rate of a substance and depends on temperature.

**Residence time.** Average time that gaseous substances spend in contact with solid compounds.

**Tar.** Condensable vapors released during pyrolysis of biomass.

**Thermogravimetric Analysis (TGA).** Thermal analysis technique that measures to high precision the mass of a sample as a function of temperature and/or time.

**TGA-MS.** Thermogravimetric analyzer coupled to a mass spectrometer.

**Volatile Matter (VM).** Gaseous and vapor substances released during pyrolysis of biomass.





# Chapter 1

## Introduction

### 1.1 Household Fuel Combustion

Nearly 50% of the world's population relies on solid fuels to fulfill their basic daily energy needs such as cooking and heating. These include traditional fuels like wood, charcoal, dung, coal and various types of agricultural waste (J-Pal Policy Briefcase, 2012). In countries like India, Haiti and most of Sub-Saharan Africa where the majority of the population resides in rural areas, more than 90% of households use traditional fuels for cooking (WHO, 2006).

The burning of these fuels is often an energy inefficient process that results in the generation of large amounts of smoke, which contains many air pollutants such as carbon monoxide, nitrogen oxides, and fine solid particles. Breathing these substances for several hours every day causes serious health problems such as chronic obstructive pulmonary disease, acute infections of the lower respiratory tract and lung cancer. In 2012, indoor air pollution was the cause of 4.3 million deaths worldwide (WHO, 2014). Women, who are in charge of cooking in most societies, and newborns and infants, who are close to the mother, are the most vulnerable.

The majority of regular solid fuel users live in poverty. In urban areas where fuels are commonly purchased, poor households typically spend a larger fraction of their income on energy needs, as compared to higher-income receiving households (Mendoza, 2011). Finances can be further challenged by seasonal effects. During the rainy

season, the price paid for solid fuels like wood and charcoal can increase up to 50% (Putti *et al.*, 2015).

Fuels like firewood can be collected, when available, in the vicinity of the household, which is frequently practiced in more rural settings. This makes the fuel free of charge, but can impose risks to the collector, such as health issues, like backaches and snake bites; safety concerns, as women living in war zones and refugee camps have experienced assault during collection; and significant time investments, approximately 60 million person years annually are needed for household fuel collection duties (Putti *et al.*, 2015).

There are also several environmental problems that arise from the utilization of solid fuels. Biomass combustion products include greenhouse gases such as carbon dioxide and methane. It has been estimated that 1.5—3.0 % of the global emissions of  $CO_2$  equivalents are related to household fuel combustion in developing countries (Olivier *et al.*, 2011). Deforestation due to wood collection for direct burning or charcoal production leads to forest degradation, erosion and soil quality decline. The use of dung as a fuel can lead to disruption of the decomposition stages of the carbon cycles and also prevent its utilization as fertilizer (Griscom *et al.*, 2009).

The United Nations, the World Health Organization and many other public and private entities have ongoing efforts to address the challenges listed above. Strategies include improved cooking devices, alternative fuels, reduction of the energetic needs, improved house ventilation, and reduction of user exposure. This work focuses in the fabrication of an alternative fuel, charcoal, from agricultural waste. It has the potential to improve indoor air quality, facilitate fuel procurement, reduce deforestation, and decrease greenhouse gas emissions.

## 1.2 Charcoal as an Alternative Fuel for Less-Resourced Settings

### 1.2.1 Wood-fuels Usage

In Sub-Saharan Africa and many other regions around the globe, wood is the most commonly used energy source in low-income households. In many Sub-Saharan African countries, over 90% of rural households and more than 50% of urban households rely on wood and wood-charcoal to satisfy their daily energy needs. The situation is similar in countries like Haiti, India, and rural areas of Latin America and South-East Asia (IEA, 2006).

Carbonizing wood to produce charcoal offers significant advantages: charcoal briquettes are smokeless, have a significantly higher energy density, and their emissions profiles are far less harmful to human health. Traditional wood-charcoal production in earth-mound kilns is practiced extensively in the developing world as it can be done with low investment costs, using locally available raw materials (Emrich, 1985). Wood-based fuel production however, has its drawbacks. Charcoal production and firewood collection typically cause forest degradation and localized deforestation (Griscom et al., 2009). In fact, a large portion of the wood utilized for charcoal production is sourced illegally from public forests, which results in over-harvesting. (World Bank, 2011).

### 1.2.2 Charcoal from Agricultural Residues

Agricultural residues can be carbonized to generate charcoal. These residues typically constitute 60-70% of the total biomass produced after harvesting (Quartey, 2008), which makes them easily accessible to low-income households that rely on agriculture as their primary source of income. Many types of agricultural residues can be used as raw materials for charcoal production, such as hazelnut shells (Demirbas, 1999), babassu nuts (Protasio *et al.*, 2014), and coffee husks (Bogale, 2009).

The carbonization of agricultural residues offers several advantages: emissions are less

detrimental to human health and contain little to no sulfur, doesn't lead to disruption of terrestrial ecosystems, can be practiced at a small scale, can lead to income generation, reduces dependence on outside fuel sources, and has zero net emissions of  $CO_2$  (Demirbas, 2001). A drawback is that briquetting and post-carbonization agglomeration processes are typically necessary, which increases operational costs (Emrich, 1985).

There is an opportunity in the growing wood-fuels markets for the introduction of charcoal made from agricultural residues, with the potential of impacting low-income households. It is estimated that household charcoal consumption in Sub-Saharan Africa will see a 50% increase in the current decade (Broadhead *et al.*, 2001). Value chains in developing nations are large and growing, and they represent an important source of income for many base-of-the-pyramid households. Millions of producers, transporters and retailers around the globe are employed in the formal and informal wood-fuel sectors in both rural and urban less-resource settings (Schure, 2012).

### **1.2.3 Fuel from the Fields: MIT D-Lab's Work**

Lead by Amy Smith, in 2002 MIT D-Lab developed an approach to making charcoal from agricultural residues for small-scale farmers that requires little capital investments and can be done using locally available materials. It can be used for household fuel production and has income-generation potential. The initial investment needed is approximately 25 USD, and the payback period if the charcoal is sold or through fuel savings is often less than one month. D-Lab's decentralized approach enables farmers to manage prices and retain profit, and also reduces transportation costs (Singh *et al.*, 2010).

The methodology developed by D-Lab typically uses corn waste or bagasse as feedstock during demonstrations, which are abundant in Sub-Saharan Africa and Haiti respectively. Carbonization is carried out using a 55 gallon metallic drum as a kiln (Figure 1-1-A), with a cost of about 15 USD per drum. Packing is done through a large hole on the top of the drum, and a wooden stick is used to create an airway to facilitate airflow (Figure 1-1-B). Ignition is done by lighting the raw materials through

smaller holes at the bottom of the drum while it's raised off of the ground with stones or bricks (Figure 1-1-C). Five to ten minutes after ignition, the gases evolved are ignitable and produce a flame, it is then when the drum is closed using a metal lid, and sand at the top and bottom to create an airtight seal (Figure 1-1-D). After the end of the carbonization process and cooling, carbonized materials are crushed, and mixed with a binder that is typically made using cassava flour and water (Figure 1-1-E). Briquettes are made by pressing the charcoal binder mixture in a simple low-cost press made of readily available steel and wood that costs approximately 2 USD and can make 10-15 briquettes per minute (Figure 1-1-F, 1-1-G). The briquettes are left out to sun dry for 3-4 days before use (Figure 1-1-H). D-Lab has trained more than 1000 people in over 20 countries on how to make charcoal from agricultural residues, and approximately 61 local producers have been established as a result of these efforts. Many community partners have taken a market-based approach and scaled up this methodology, while several others are working on dissemination (Fuel from the Fields Charcoal Do It, n.d.).

This work focuses on the characterization of the carbonization of corn agricultural residues. Non-isothermal pyrolysis of the corn husks, stalks and cobs was carried out in the furnace of a Thermal Gravimetric Analyzer at different heating rates to derive proximate analysis data and kinetic parameters for each material. A Mass Spectrometer was coupled to the furnace to obtain qualitative insight of the gaseous products. This data aims to improve the current understanding of charcoal fabrication practices in the field, and facilitate technology transfer between D-Lab's Clean Fuel Research Group and its community partners.

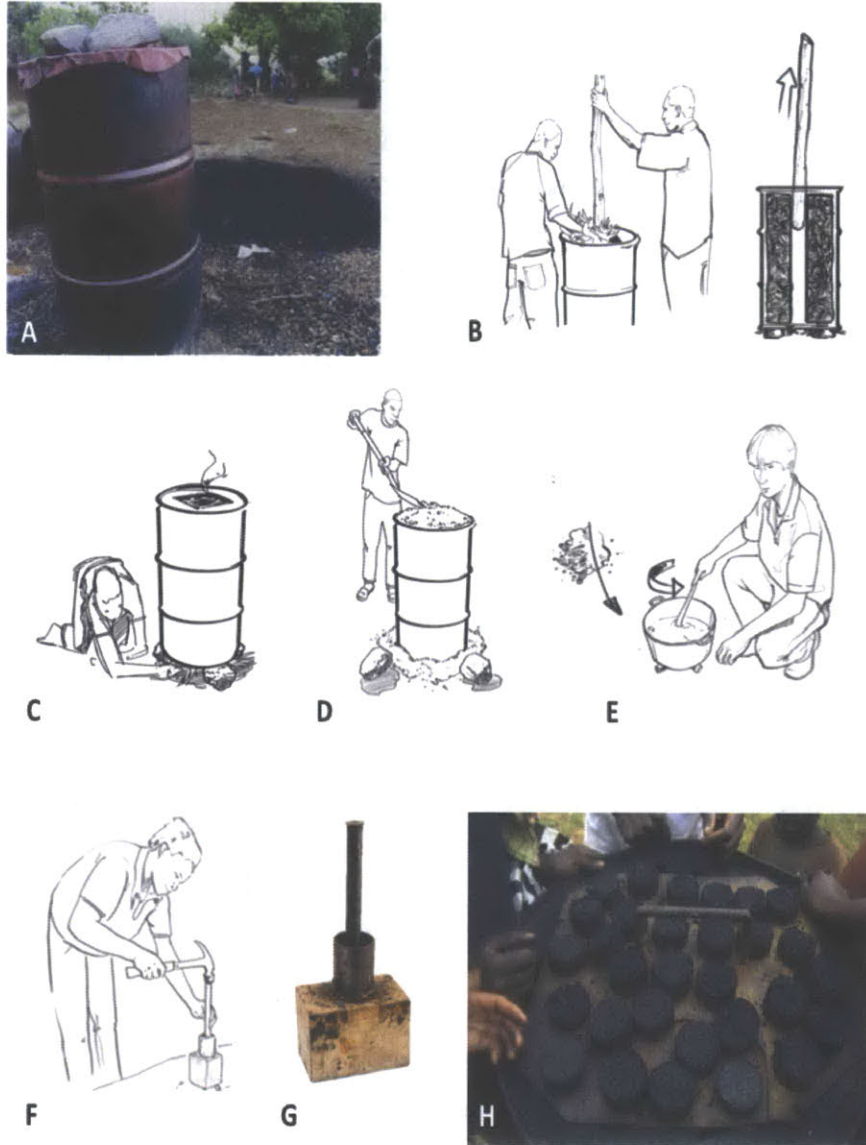


Figure 1-1: MIT D-Lab Charcoal Process. A. 55 gallon drum used as kiln. B. Material packing. C. Ignition. D. Sand based air-tight seal. E. Binder making. F. Pressing of briquettes. G. Briquette Pressing Technology. H. Briquettes before drying. Copyright ©Massachusetts Institute of Technology. Accessed on Nov 20, 2015.

# Chapter 2

## Experimental Design

This chapter describes the thermochemical considerations necessary for the design of the experimental methodology, and also details the materials and methods used in this work.

### 2.1 Biomass Composition

#### 2.1.1 Ligno-cellulosic Composition of Herbaceous Biomass

A large portion of agricultural waste is categorized as herbaceous biomass, which is composed primarily of ligno-cellulosic materials. These are materials composed predominantly of three polymers: cellulose, hemicellulose, and lignin. Cellulose is a linear homopolysaccharide that represents 30-50% of dry feedstock matter by mass. It is the most common organic compound on earth and provides skeletal structure. Cellulose decomposes at 320 °C. Hemicellulose is a polyose that constitutes 20 to 40% of feedstock dry matter. It is composed of short, highly branched polymers and has an amorphous structure with little strength. It decomposes between 200 °C and 260 °C. Lignin is a highly-branched polyphenolic polymer that constitutes 15-20% of the dry feedstock. It is structural to plants and decomposes between 280 °C and 500 °C, with rapid decomposition above 320 °C (Demirbas, 2001).

Corn stover describes all of the biomass that comes from corn and grows above the

ground, except for the grain. It includes stalks, leaves, tassel, husk and cobs. Corn stover is composed of approximately 38% cellulose, 26% hemicellulose and 19% lignin (Lee *et al.*, 2007). The ligno-cellulosic composition of corn stover also varies according to its source within the plant (Liu *et al.*, 2015). To account for the ligno-cellulosic composition variations and better understand their impact in carbonization processes, three samples of corn were studied: cobs, husks, and stalks.

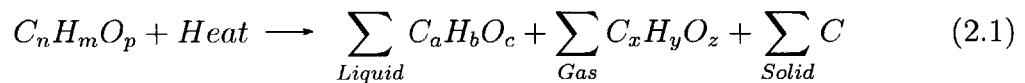
### 2.1.2 Proximate Analysis

Analytical methods for the determination of biomass composition in terms of cellulose, hemicellulose and lignin are often of high complexity and require expensive equipment (Parikh, 2007). Proximate Analysis is a useful, easy-to-measure, and widely used method for characterizing the gross composition of biomass by mass percentage of moisture, volatile matter, ash, and fixed carbon (Basu, 2013).

## 2.2 Pyrolysis and Thermal Analysis

### 2.2.1 Overview of Pyrolysis and Decomposition Kinetics

Pyrolysis refers to the thermochemical decomposition of biomass in temperatures of 380 °C to 650 °C and pressures of 0.1 MPa to 0.5 MPa under an inert atmosphere. Carbonization processes are a type of slow pyrolysis, which are characterized by slow heating rates, and long residence times, and are used around the world for traditional charcoal production (Basu, 2013). The process can be described by the following reaction:



The solid yield of pyrolysis is known as charcoal, a black non-lustrous residue, composed largely of amorphous elemental carbon, and small quantities of ash (Ency-



lopedia Americana, 1994). The liquid yield, also known as tar, is a black fluid that is composed of hydroxyaldehydes, hydroxyketones, sugars, carboxylic acids, and phenolic compounds. The gaseous products, are a mixture of low molecular weight non-condensable gases like carbon dioxide ( $CO_2$ ), carbon monoxide (CO), methane, ethane and ethylene; and other condensable secondary gases (Basu, 2013).

The mechanisms through which ligno-cellulosic materials undergo decomposition reactions over time are tremendously complex. Many researchers have created simplified models to understand behavioral trends instead of reaction specifics for biomass pyrolysis. The First Order Global Single Reaction Model (Stamm, 1956), approximates pyrolysis as an irreversible single first-order reaction, as described by the equation:



Based on these assumptions, the mass loss rate can be modeled as:

$$\frac{dm_b}{dt} = -k(m_b - m_c) \quad (2.3)$$

where  $m_b$  is the mass of biomass in  $kg$ ,  $m_c$  is the mass of char after pyrolysis in  $kg$ ,  $t$  is time in  $s$ , and  $k$  is the reaction rate in  $s^{-1}$ .  $k$ 's temperature dependence is given by the Arrhenius equation:

$$k = A \cdot \exp\left(\frac{-E_a}{RT}\right) \quad (2.4)$$

where  $A$  is the pre-exponential coefficient in  $s^{-1}$ ,  $E_A$  is the activation energy in  $Jmol^{-1}$ ,  $R$  is the gas constant in  $Jmol^{-1}K^{-1}$  and  $T$  is temperature in  $K$ .

This model assumes a fixed mass ratio between pyrolysis, does not differentiate between condensable and non-condensable gases, and overlooks the multi-step nature of decomposition processes. For charcoal production applications however, where the solid char product is of foremost interest, it can provide a guide for the characterization of a given material. Data for the pre-exponential factor  $A$  and the activation Energy  $E_a$  assuming a first order kinetic model has been published to characterize various types of biomass, including corn stalks (Zabanitou & Ioannidou, 2008).

## 2.2.2 Thermogravimetric Analysis

Thermogravimetry is an analytical technique that is widely used to study the properties of biomass. A thermogravimetric analyzer, or TGA, consists of a pan that is connected to an analytical balance, which records the mass loss of a sample when exposed to a temperature profile under a controlled gaseous environment. TGA is a reliable technique that can provide information about the complex behavior that biomass exhibits during decomposition (Yang *et al.*, 2006).

Data obtained from TGA is typically represented graphically, as shown in Figure 2-1. The thermogravimetric curve (TG) is a plot of the sample's percentage of absolute mass versus temperature or time, as shown in orange in Figure 2-1. The derivative-thermogravimetric curve, DTG, shows the derivative of the TG curve with respect to temperature or time, and is shown in blue. Biomass decomposition zones can be easily identified from a TG-DTG curve. Labeled as A, between room temperature and 110 °C is the moisture loss zone, where the sample releases water and other low boiling point gases. Under an inert atmosphere and standard pressure, pyrolysis occurs between 200 °C and 600 °C. The pyrolysis zone, labeled as B, corresponds to a sudden drop in mass due to the rapid release of volatile matter, a product of biomass decomposition. Labeled as C, between 600 °C and 800 °C is the char zone. In the char zone, the material left is composed of carbon and ash only.

The percentage mass lost in each zone can be used to obtain proximate analysis data for a sample (Gabbott, 2008). In this work, Proximate Analysis was obtained by integrating the DTG curve for each zone. The MATLAB code utilized to do so can be found on Appendix A. Ash and Fixed Carbon content were grouped into a single value referred to as char percentage, which is a measure of char yield. This was done because corn stover contains overall percentages of ash in its structure of about 6% (Lee *et al.*, 2007) that are consistent with typical ash contents in charcoal for cooking (Emrich, 1985). Char yield was calculated at 700 °C and 900 °C.

TGA data can also be used to calculate the pre-exponential coefficient,  $A$ , and the activation energy,  $E_a$ . Flynn & Wall created a method for calculating  $E_a$  by plotting

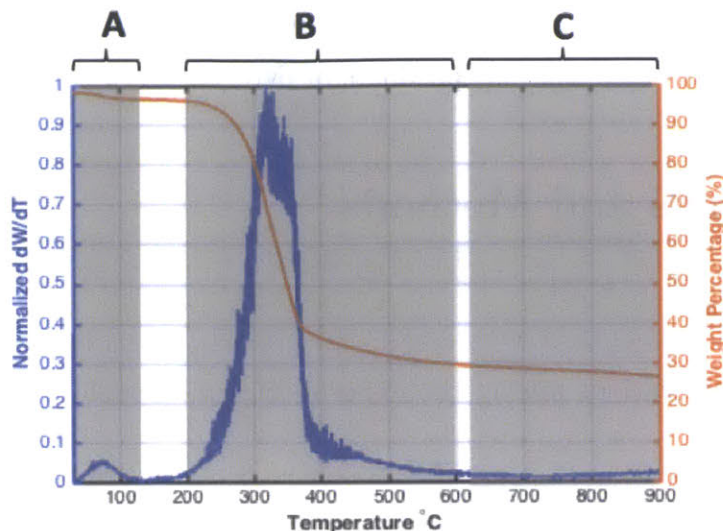


Figure 2-1: Stages of biomass pyrolysis in a TG-DTG curve. A. Moisture loss zone. B. Pyrolysis zone. C. Char zone.

the heating rate as a function of the negative reciprocal absolute temperature for equivalent mass loss percentages for two or more constant heating rates (Flynn & Wall, 1966). In this work, this method was utilized in the pyrolysis regime of the temperature profile. Variants of the Cats-Redfern linearization method, proposed by Zsako *et. al* in 1980 are used for the calculation of  $A$  (Zsako & Zsako, 1980). Zsako's method offers tabulated data for a range of activation energies and temperatures, and allows for evaluation of accuracy by estimation of apparent activation energy values. The MATLAB code utilized for the calculation of  $E_a$  and  $A$  can be found on Appendix A.

$A$  and  $E_a$  provide quantitative information about the relative amounts of char and volatiles throughout the course of the reaction with respect to their initial concentration, which is useful for determining char yield at any given time, for example. However, they fail to provide qualitative information about the nature of the species generated during decomposition. TGA can be coupled to a Mass Spectrometer, in a technique referred to as TGA-MS, to provide information of the nature of the volatile matter produced. By measuring the mass-to-charge ratio ( $m/z$ ) and abundance of a

gaseous substance's ions, mass spectrometers can very accurately identify the nature and relative amounts of the gaseous products of pyrolysis (Tiwari & Deo, 2012).

## 2.3 Materials and Methods

### 2.3.1 Strategy

Based on the considerations above, the experimental methodology was designed to meet two objectives:

1. to experimentally obtain mass loss data as a function of temperature for the pyrolysis of corn cobs, husks and stalks,
2. to obtain qualitative data about the emissions profile of corn cobs, husks and stalks during pyrolysis.

In order to accomplish these objectives, three types of experiments were carried out:

- **Experiment 1.** TGA data was obtained for corn cobs, husks, and stalks samples to characterize their thermal decomposition. The mass loss data obtained was used to calculate the sample's proximate analysis.
- **Experiment 2.** TGA-MS data was obtained for corn cobs, husks, and stalks samples to characterize their thermal decomposition and obtain compositional information about the volatile products generated during pyrolysis. The mass loss data obtained was used to calculate sample's proximate analysis. The spectral data was used to understand the emission patterns on  $H_2O$ ,  $CO$ ,  $H_2S$  and aromatic compounds.
- **Experiment 3.** The rate of temperature increase as a function of time affects reaction pathways and kinetics. TGA data was obtained for corn cob and husk samples to characterize their thermal decomposition process at higher heating rates. The mass loss data obtained was used to calculate the sample's proximate analysis, pre-exponential constant,  $A$ , and activation energy,  $E_a$ .

### 2.3.2 Material Preparation

Air-dried stalk, husk, and cob samples from a farm near the Boston area were used in this study. No chemical pre-treatment was performed prior to measurement. 150 g of corn stalks (Figure 2-2-A) were cut with a knife into pieces of approximately 15 cm in length, and then put in a Hamilton Beach Big Mouth Duo Deluxe 14 food processor for 5 minutes. The processed material was sieved first with a #5 mesh (4000  $\mu\text{m}$ ) sieve and then with a #35 mesh (500  $\mu\text{m}$ ) to reduce temperature gradients within the sample. 20 g of dry corn husks (Figure 2-2-B) were selected to avoid presence of fungi or other contamination. Stalks were cut away to ensure the sample contained husks only and then put in a Hamilton Beach Big Mouth Duo Deluxe 14 food processor for 3 minutes. The obtained material was sieved as with stalk samples. 13 corn cobs were collected and sliced into sections of approximately 1 cm thickness with a band saw (Figure 2-2-C). These slices were crushed using a hand operated mill (Figure 2-2-D). The obtained material was sieved as before.

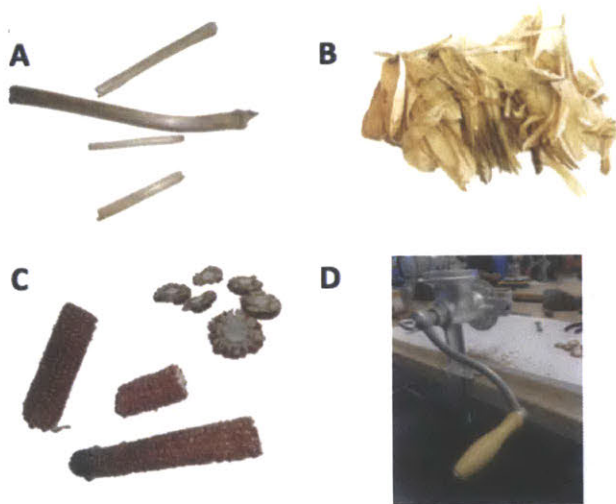


Figure 2-2: Corn stover samples and mill. A. Corn stalk. B. Corn husks. C. Corn cobs. D. Hand operated mill used for cob's processing.

### 2.3.3 Experimental Set-up

A TA Instruments Discovery Thermogravimetric Analyzer Model TGA1-0075 was coupled to a Prisma QMS 200 Mass Spectrometer by Pfeiffer (Figure 2-3). All samples were tested on 100  $\mu$ L high temperature platinum pans. For all experiments, the system was allowed to stabilize at 30  $^{\circ}$ C, before starting the temperature ramp with a heating rate specified on Table 1. All samples were tested up to 900  $^{\circ}$ C to prevent residual tars and oils from affecting the solid yield. Experiment 1 was conducted under an inert atmosphere of Nitrogen ( $N_2$ ). Helium ( $He$ ) was used as the carrier gas for experiments 2 and 3 for compatibility with mass spectrometer. For TGA-MS the samples were flushed with Helium for 5 hours at a mass flow of 200 mL/min to completely clean the spectrometer. The conditions of the experiments conducted are summarized in Table 2.1.

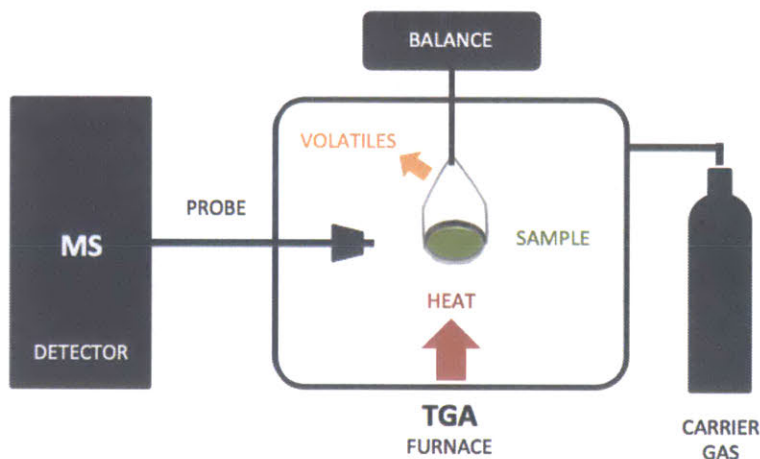


Figure 2-3: TGA-MS Experimental Set-up

Table 2.1: Detail of samples and experiments performed

Experiment	Sample ID	Material	Heating Rate (°C/min)	Carrier Gas
1	C-1	Cob	20	$N_2$
1	H-1	Husk	20	$N_2$
1	S-1	Stalk	20	$N_2$
2	C-2	Cob	2	$He$
2	H-2	Husk	2	$He$
2	S-2	Stalk	2	$He$
3	C-3	Cob	10	$He$
3	H-3	Husk	10	$He$





# Chapter 3

## Results and Discussion

### 3.1 TG-DTG Curves

TG-DTG curves were successfully obtained for all samples. They showed two major features: pyrolysis loss and moisture loss. The most significant mass loss due to volatile matter release during pyrolysis was observed between 200°C and 400°C for all materials, as indicated by the increased absolute value in their respective DTG curves. A smaller, but appreciable increase in water loss rates around 100 °C was observed for all materials as well, corresponding primarily to moisture loss.

### 3.1.1 Corn Cobs

The TG-DTG curve for sample C-1 is shown in Figure 3-1. Maximum conversion rates were observed at 320 °C, and a secondary less defined peak between 335 °C to 370 °C was also observed. The maximum rate likely corresponds to cellulose decomposition (Li *et al.*, 2008). The secondary peak could correspond to ligning decomposition. The shoulder before the maximum peak, between 240 °C and 280 °C, likely corresponds to hemicellulose decomposition, which is known to occur at lower temperatures than cellulose's (Yang *et al.*, 2006). Sample C-2 showed maximum conversion rates at 340 °C, as it can be seen in the DTG curve of Figure 3-2. Sample C-3 showed maximum pyrolysis conversion at 345 °C, and a secondary peak at 365 °C, similarly to C-1. Secondary peaks appear due to changes in the kinetics of decomposition.

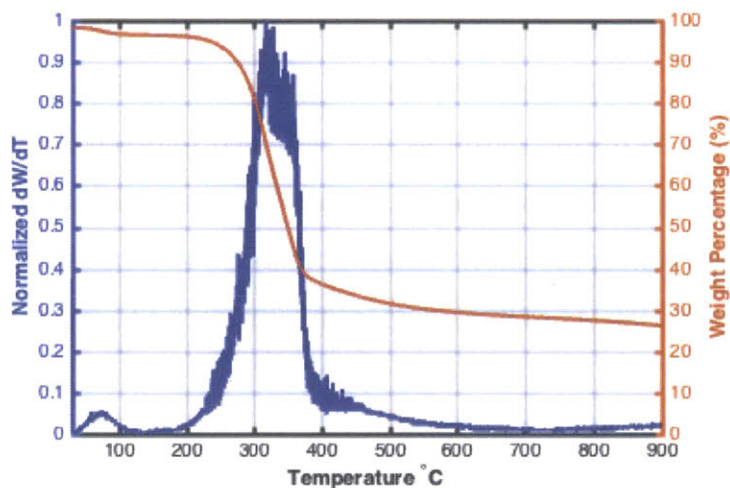


Figure 3-1: TG-DTG curve for corn cob sample C-1 with heating rate 20 °C/min

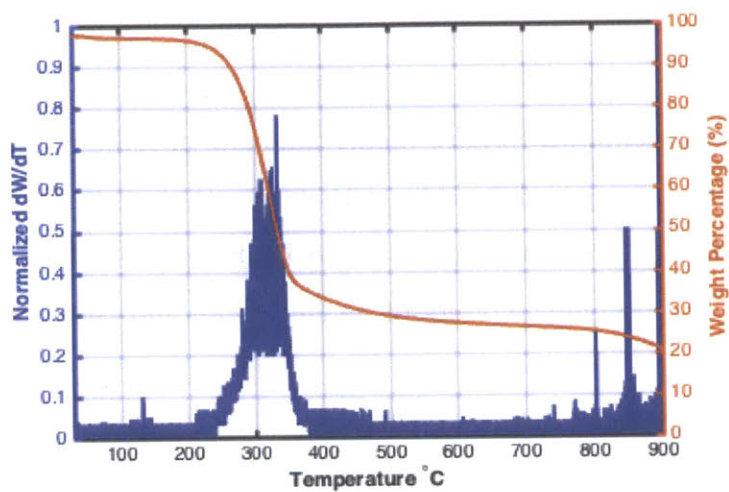


Figure 3-2: TG-DTG curve for corn cob sample C-2 with heating rate 2 °C/min

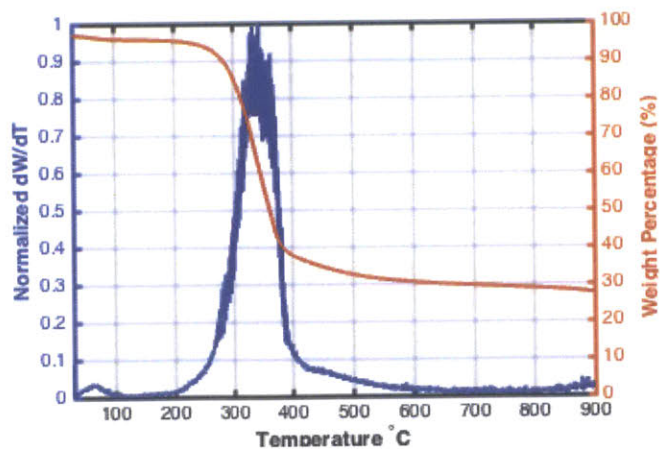


Figure 3-3: TG-DTG curve for corn cob sample C-3 with heating rate 10 °C/min

### 3.1.2 Corn Husks

DTG curves for corn husk samples (Figures 3-4, 3-5 and 3-6) showed defined doublets in the cellulose and hemicellulose rapid decomposition zones, with maximums for H-1 at 320 °C and 265 °C, for H-2 at 300 °C and 340 °C, and for H-3 at 320 °C and 365 °C. Corn husks are known to have higher amounts of cellulose and hemicellulose in their structure as compared to cobs and stems (Sinha *et al.*, n.d.). A higher initial concentration of both substances could expedite the differentiation of their decomposition zones. Larger amounts of hemicellulose and cellulose, which readily decompose into gases, are present in husks as compared to other materials (Barten, 2013). This behavior matches that modeled and observed for corn husks by Li. *et al.*

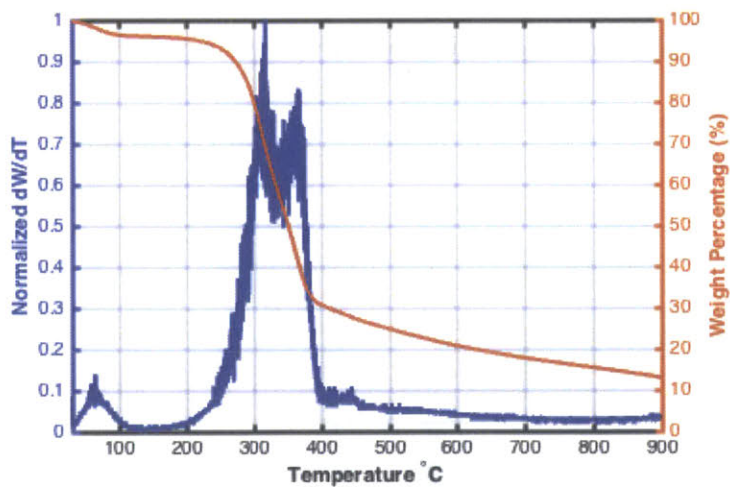


Figure 3-4: TG-DTG curve for corn husk sample H-1 with heating rate 20 °C/min

Figure 3-5: TG-DTG curve for corn husk sample H-2 with heating rate 2 °C/min

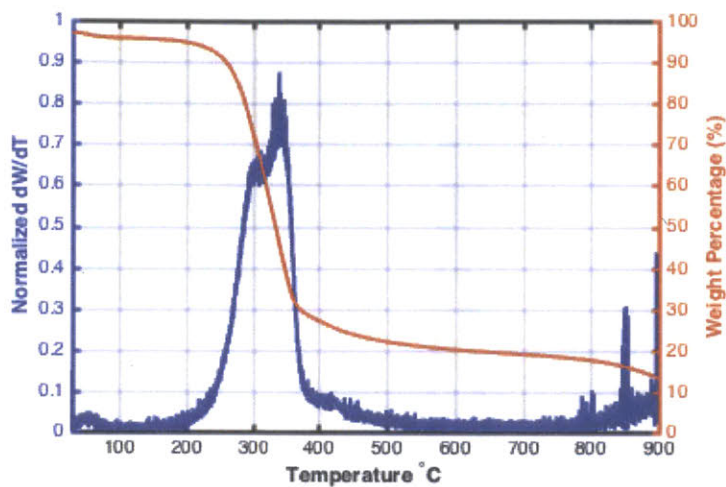
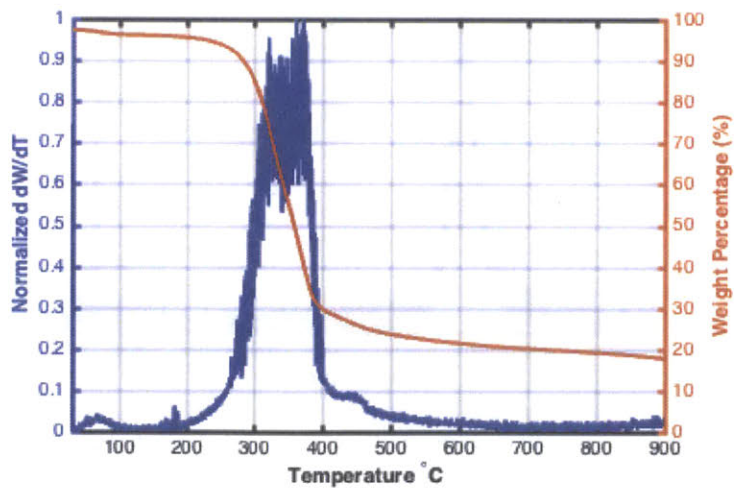


Figure 3-6: TG-DTG curve for corn husk sample H-3 with heating rate 10 °C/min



### 3.1.3 Corn Stalks

TG-DTG curves for corn stalk samples S-1 and S-2 are shown in Figures 3-7 and 3-8, respectively. They showed a single maximum peak in the pyrolysis zone, at 330 °C for S-1, and 310 °C for S-2.

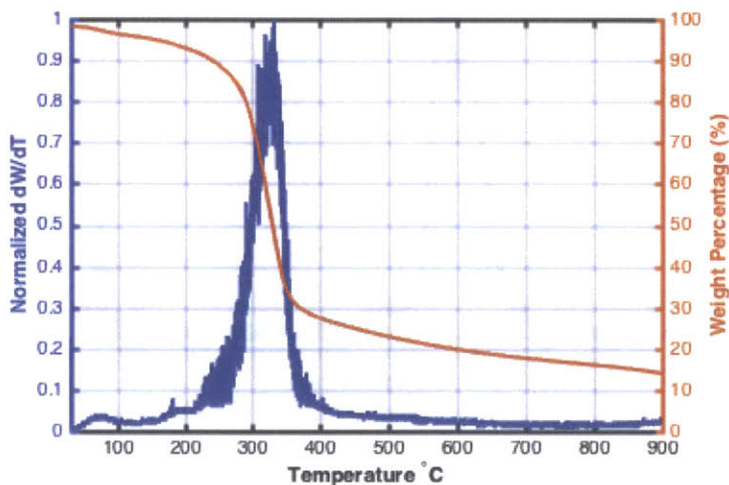


Figure 3-7: TG-DTG curve for corn stalk sample S-1 with heating rate 20 °C/min

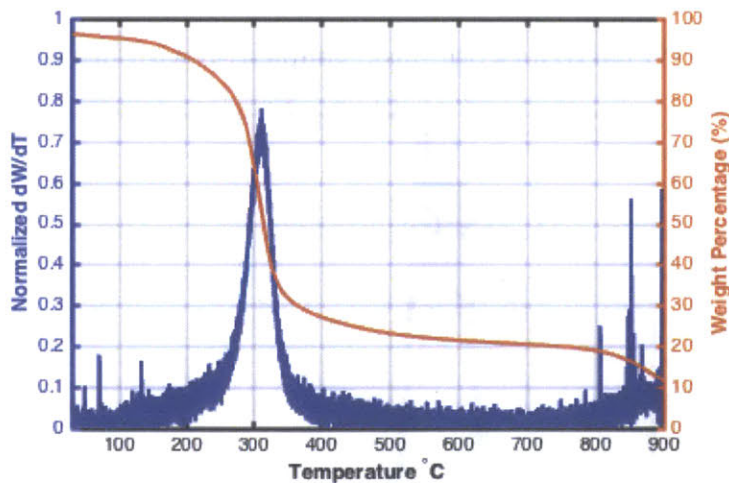


Figure 3-8: TG-DTG curve for corn stalk sample S-2 with heating rate 2 °C/min

### 3.1.4 Comparisons Between Experiments 1 and 2

Pyrolysis temperatures significantly impact conversion. In both experiments, corn husks showed pyrolytic gas release over a larger temperature range, as it can be observed in the DTG curves of Figure 3-9. Stalks on the other hand, showed maximum volatile matter release across a smaller temperature range. Corn stalks began pyrolysis at lower temperatures and slower rates than cobs and husks, as shown in the TG curves of Figures 3-9, which could contribute to the decrease of pyrolysis rates at lower temperatures. Hemicellulose decomposition has lower activation energy than cellulose and occurs between 200 °C and 260 °C. Therefore corn stalks with larger hemicellulose mass percentages would explain this behavior.

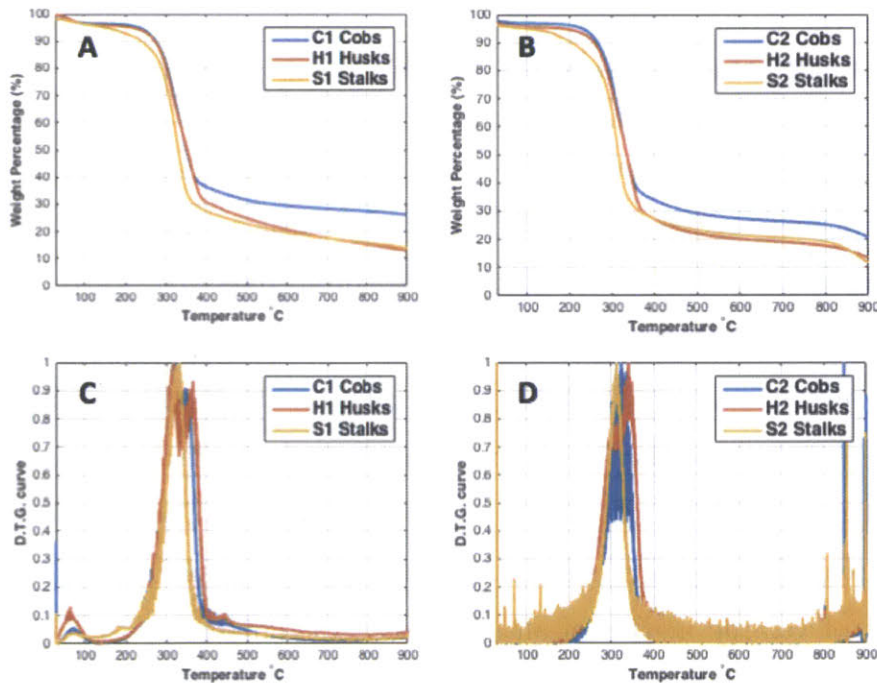


Figure 3-9: TG and DTG curves for Experiments 1 and 2. A. TG curves for Experiment 1 samples C-1, H-1 and S-1. B. TG curves for Experiment 2 samples C-2, H-2 and S-2. C. DTG curves for experiment 1 samples C-1, H-1 and S-1. D. DTG curves for experiment 2 samples C-2, H-2 and S-2.

In both experiments, before and during conversion, cob and husk samples had similarly shaped TG curves, which indicates they have similar decomposition kinetics. This is supported by the fact that their hemicellulose, cellulose and lignin composition ratios are very similar (Liu *et al.*, 2015). There is a difference at the end of the pyrolysis zone close to 400 °C, where cobs cease pyrolysis while husks continue to decompose. This can be explained by the the larger percentage of fixed carbon that cobs typically present (Lee *et al.*, 2007).

DTG peaks were less distinguishable in experiment 2 when compared to experiment 1. This is because decomposition of various constituents occurred simultaneously and caused peak overlapping (Haykiri-Acma *et al.*, 2006).

## 3.2 Proximate Analysis and Char Yield

Proximate analysis values were calculated from mass loss data and are shown in Table 3.1. Proximate analysis values for moisture, volatile matter, and charcoal of all samples match literature-reported values (Zabaniotou, 2008).

Moisture content at the time of carbonization is one of the most important factors influencing conversion yield (Emrich, 1985). High moisture content materials can't be used as fuel directly in thermo-chemical processes, as increased moisture content lowers calorific value. Husk and stalk samples in experiments 1 and 2 showed higher moisture content than that of cobs. In all experiments, cob samples also showed the least amount of volatile matter of all samples, with a difference of 7% by mass or more when compared to husks and stalks. The percentage of charcoal, which in this case was a measure of char yield, showed to be higher for cobs in all experiments as well.

A high yield means that less agricultural waste is needed for the same amount of charcoal obtained, which impacts the amount of material that needs to be dried, transported, and loaded in the carbonization unit. These findings suggest that cobs are best suited as feedstock for charcoal production than stalks and husks.



Table 3.1: Proximate analysis for corn stover samples from TGA data

Sample	Moisture (%)	Volatile Matter (%)	Charcoal at 900°C (%)	Charcoal at 700°C (%)
C-1	2.36	66.45	26.67	28.84
H-1	4.34	78.24	12.95	17.79
S-1	3.11	74.40	14.29	17.98
C-2	1.49	61.63	21.00	26.95
H-2	1.61	73.87	13.68	19.59
S-2	2.37	67.87	11.97	21.31
C-3	1.85	64.98	28.28	30.37
H-3	1.56	74.54	18.17	20.65

### 3.3 Emissions from Mass Spectroscopy

For experiment 2, four mass-to-charge ratios ( $m/z$ ) corresponding to the following species were analyzed: 18, for  $H_2O$ ; 28, for  $CO$ ; 34, for  $H_2S$ ; and 34, for  $C_4H_2$ . These compounds are relevant to pyrolysis and their relative abundance as given by the intensity as a function of the temperature profile resulted in relevant and easy to analyze data for emissions.

The abundance of water, assumed to correspond to fragment  $m/z = 18$ , as shown in Figure 3-10, was observed to increase both at the moisture release zone, and pyrolysis zone. The maximum for pyrolysis is at 220 °C, in the cellulose peak decomposition zone. The abundance increase in the pyrolysis zone corresponds to dehydration of the ligno-cellulosic components of biomass (Koppmann *et al.*, 2005). For the husk samples, a bimodal trend can be observed, where hemicellulose dehydration creates a shoulder at 220 °C and cellulose degradation creates the maximum abundance peak at 340 °C. A decrease in the water fragment abundance was observed to intensify between 800 °C and 900 °C. It is possible that moisture present in the carrier gas or entering the furnace due to a leak reacted with carbon at these temperatures.

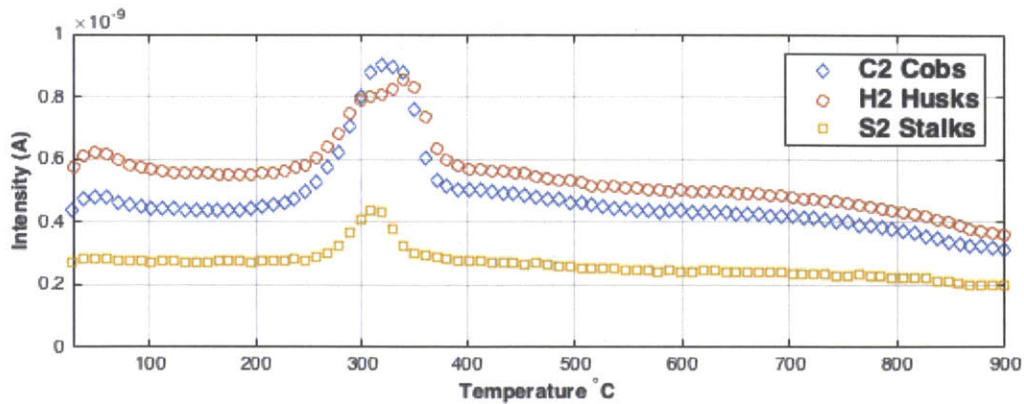


Figure 3-10: Abundance as a function of TGA temperature profile for  $m/z = 18$

The 28  $m/z$  fragment was studied for representing CO, an important indoor air quality indicator, but could also refer to the presence of ethylene and  $N_2$ . For all three samples its abundance increases in the pyrolysis zone as expected, as shown in Figure 3-10. For stalks and husks however, the background presence of this fragment is an indicator of insufficient purge in the instrument. The increase in relative abundance of this fragment between 800 °C and 900 °C supports the possibility of mass loss due to fixed carbon oxidation reactions, which shouldn't be observed at this temperatures (Gabbott, 2008), unless there is an oxygen leak in the instrument. Due to this, the char yield was calculated at 700 °C and 900 °C.

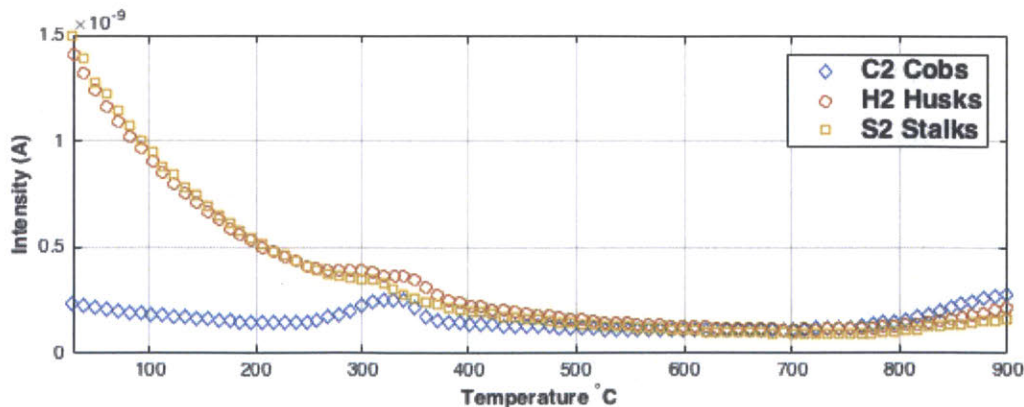


Figure 3-11: Abundance as a function of TGA temperature profile for  $m/z = 28$

The 34  $m/z$  fragment corresponding to  $H_2S$ , chosen to characterize sulfur emissions, showed a lower overall abundance as compared to previously analyzed fragments. Figure 3-11 shows that corn cobs and husks produce more emissions of this gas than stalks. Further studies are needed to confirm this trend.

The 50  $m/z$  fragment is a good indicator of aromatic compounds. Figure 3-12

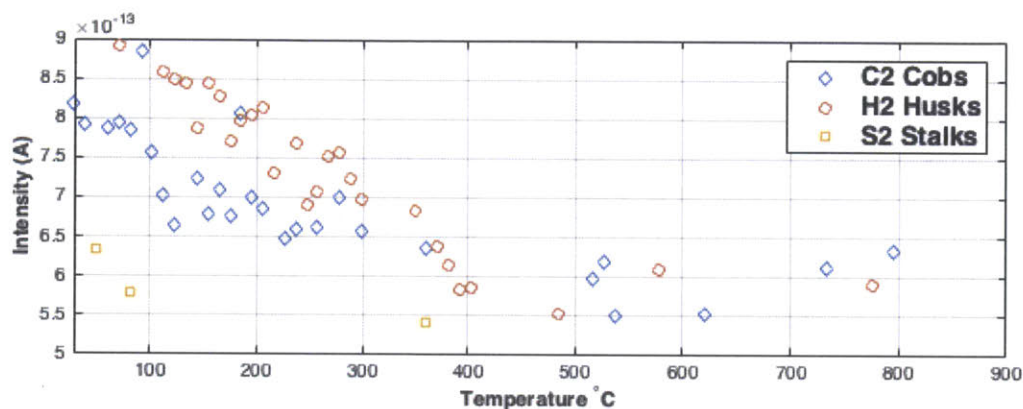


Figure 3-12: Abundance as a function of TGA temperature profile for  $m/z = 34$

shows its presence in the pyrolysis zone, between 280 °C and 240 °C for husk samples, and 300 °C and 500 °C for cob samples. Cob samples showed a larger frequency of this compound. Further work is needed to understand this behavior. Specifically, an instrument with sensing capabilities for higher  $m/z$  ratios is required.

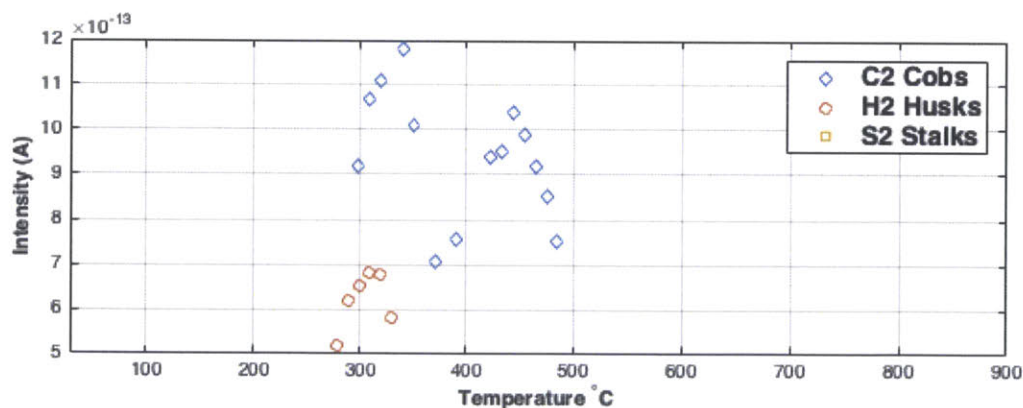


Figure 3-13: Abundance as a function of TGA temperature profile for  $m/z = 50$

### 3.4 Effect of Heating Rate

Heating rates can significantly impact decomposition kinetics. As expected, decomposition temperature ranges were higher with increased heating rates, as it can be observed in Figure 3-14. This is due to the increase in energy available per unit time (Mani *et al.*, 2010).

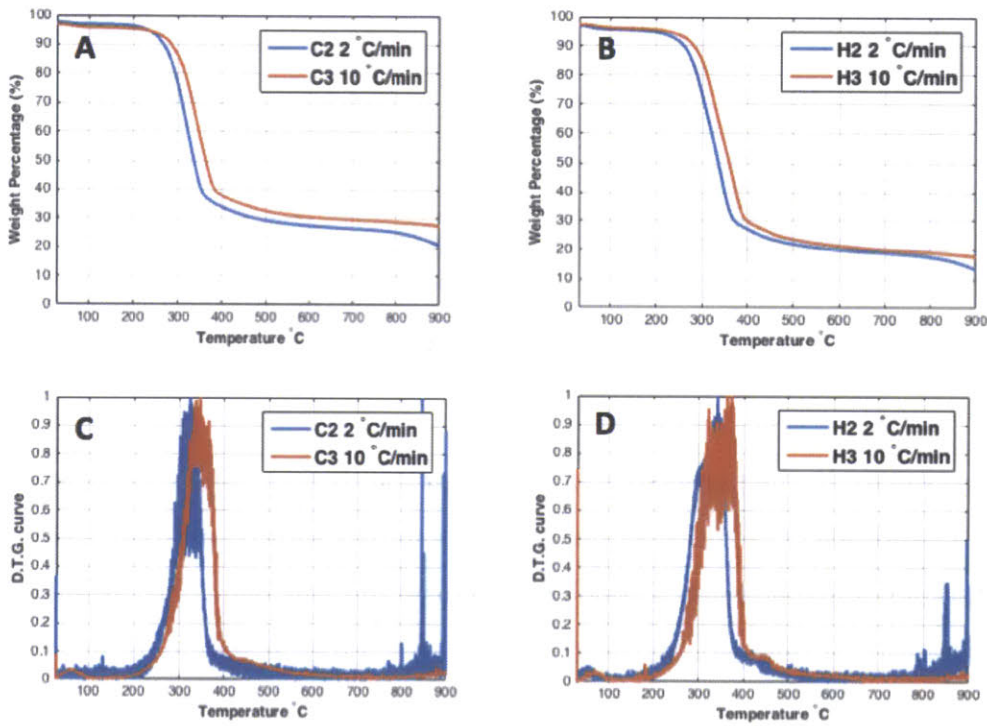


Figure 3-14: TG and DTG curves for Experiments 2 and 3. A. TG curves for Experiment 2 samples C-2 and H-2. B. TG curves for Experiment 3 samples C-3, H-3. C. DTG curves for experiment 2 samples C-2, H-2. D. DTG curves for experiment 3 samples C-3, H-3.

Slower heating rates typically maximize char production. In this case this trend can be observed in column 5 on Table 3.1, when char yield was calculated at 700 °C, before carbon reacted with oxygen from a potential leak in the instrument. When calculating char yield at 900 °C however, experiment 2 shows lower percentage yield. This unexpected behavior can be explained by the carbon oxidation reactions between 800 °C and 900 °C, which make the char yield unrepresentative at 900 °C.

### 3.5 Determination of $E_a$ and $A$

The slope of a plot of the natural logarithm of the heating rate vs. the reciprocal absolute temperature was used for the calculation of activation energies using the method by Flynn *et al.*, and are shown in Figures 3-15 and 3-16. The results obtained for  $E_a$  and the pre-exponential factor  $A$  are shown in Table 3.2.

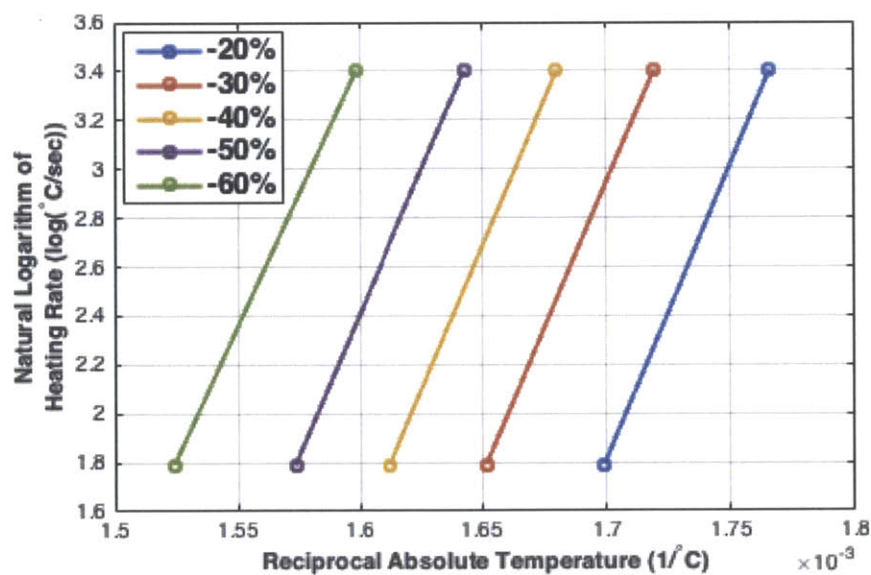


Figure 3-15: Logarithm of heating rate vs. reciprocal absolute temperature for equivalent mass percentage losses of cob samples at 2 °C/min and 10 °C/min

Table 3.2: Kinetic parameters obtained for corn cobs and husks pyrolysis

Sample	Pre-exponential coefficient ( $s^{-1}$ )	Activation Energy (KJ/mol)
Cob	1.3E5	88.6
Husk	5.2E5	96.4

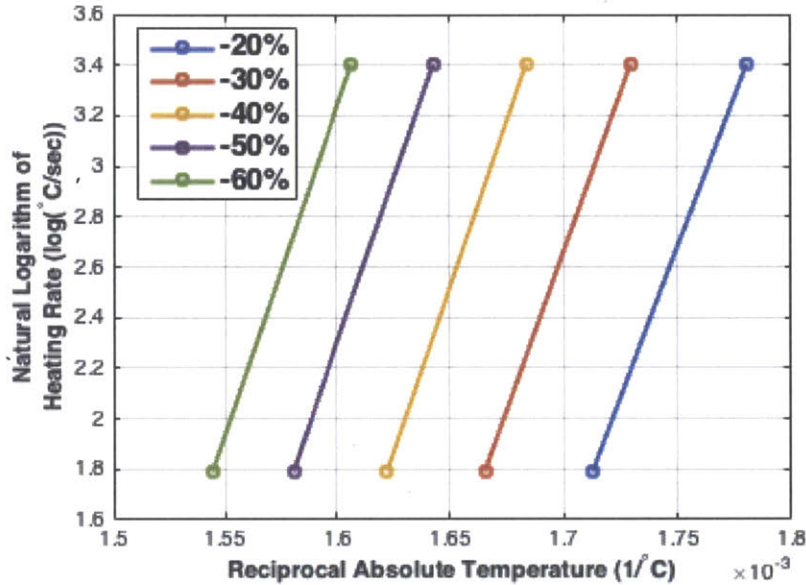


Figure 3-16: Logarithm of heating rate vs. reciprocal absolute temperature for equivalent mass percentage losses of husk samples at 2 °C/min and 10 °C/min

Values obtained for  $E_a$  and  $A$  were similar to those reported by literature for the volatile matter release zone for corn stover materials at similar heating rates (Lanzeta & Di Blasi, 1998). Specifically, for cob samples, the  $E_a = 88.6 \text{ kJ/mol}$  falls within the ranges found by Aboyade *et. al* in 2011 for heating rates between 10 °C/min and 50 °C/min. Corn husk's  $E_a = 96.4 \text{ kJ/mol}$  is similar to that reported by Li *et al.* in 2008 for a reaction order of one and 20 °C/min heating rates. Pre-exponential factors  $A$  are lower than those reported by both authors, which is expected due to the lower heating rates used in this study. These results suggest that the methodology utilized for their calculation is effective and can potentially be applied to other materials. Corn husks showed a larger activation energy than cob samples. A larger value for the

activation energy implies that more energy is needed to drive the pyrolysis reaction, which would translate to larger initial temperatures needed for the carbonization of husks. This is another reason that supports the utilization of cobs for charcoal production. Further work with a larger number of heating rates needs to be done to confirm this theory.

### 3.6 Other Considerations

The effect of particle size was assumed to be insignificant in this work, as all samples were sieved to comparable sizes. This aspect however, needs to be taken into account for work in the field, where no crushing will occur before conversion. Larger particles can promote secondary cracking and therefore result in better yields, whereas finer particles allow for gases to easily escape, which promotes larger liquid yields (Demirbas, 2001). This indicates that the utilization of uncrushed feedstock is best for maximizing charcoal yields. It has also been shown that smaller particles result in lower fixed carbon contents and lower calorific values (Bridgeman *et al.*, 2007). Samples tested in this study are expected to follow this behavior.

For this work, the corn stover was allowed to air dry for long periods of time until all surface moisture was removed, and only inherent moisture remained. In real applications however, there is a trade-off between air drying to reduce moisture, and loss of wood due to biological deterioration due to insect attack or decay (Emrich, 1985).





## Chapter 4

# Worksheet for Char Yield Monitoring

With the objective of supporting D-Lab's field work carbonization exercises, a worksheet for char yield was created.

In page 1 (Figure 4-1), it provides a simple explanation of the stages of the carbonization process, easy to observe parameters such as color and time to identify each stage, and space for recording time and weight results for 10 charcoal burns. It uses initial and final weight to calculate char yield.

Page 2 (Figure 4-2) provides instructions for use and a table for recording burn conditions. By comparing char yields for various burns with different conditions in the field, the impact of said conditions can be evaluated. This aims to facilitate informed improvement in the burn's methodology.

The worksheet has a simple format that reduces utilization of ink, and is available as a Microsoft Word 97 document to ensure compatibility and allow for improvement.

### CHARCOAL BURN: Timeline and Yield Log

#	STAGE	TIME (MIN)	TEMP (°C)	FEATURES	DESCRIPTION	Record	BURN													
							1	2	3	4	5	6	7	8	9	10				
1	Initial weight	0	r.t.	Measure weight of dry material.	Measure weight of initial materials only.	Weight														
2	Ignition	0 - 2	r.t.	Set material on fire.	Combustion of biomass to generate heat.	Time														
3	Heat absorption	2 - 5	20 - 110	Smoke. Drum gets hotter.	Biomass absorbs heat and begins to release water.	Time														
4	Drying	5 - 10	90 - 110	White, cloudy smoke.	All water evaporates from biomass.	Time														
5	Ignitable gases	10 - 15	110 - 300	Gas lights on fire. Lighter, darker, smoke.	Exothermic decomposition begins.	Time														
6	Seal	15 - 16	110 - 300	Use sand to seal drum.	Creates inert atmosphere for carbonization.	Time														
7	Carbonization	16 - 90	300 - 400	Drum stays hot.	Material carbonizes.	Time														
8	Cooling	90 - 180	300 - 400 to r.t.	Drum cools down.	Carbonization is complete.	Time														
9	Final weight	180	r.t.	Measure final weight.	Measure weight of final carbonized materials only.	Weight														
10	Char Yield	$Yield = \frac{Weight\ initial}{Weight\ final} \times 100\%$				Yield														

Figure 4-1: Charcoal burn worksheet Page 1.

## CHARCOAL BURN: Timeline and Yield Log

**OBJECTIVE.** This worksheet aims to facilitate the analysis of conditions that result in larger charcoal production for a burn. It has simple explanation of the stages of a burn, and allows for the calculation of *char yield*, a measure of how much charcoal was produced as a function of the initial biomass quantity. Higher char yield means better performance.

**MATERIALS.** To use it, you will need (1) A clock, watch or phone to record time, (2) a scale or balance, to record weight, and (3) a calculator

**TERMINOLOGY.** *Biomass.* Plants or agricultural waste used as source of energy. *Carbonization:* Process of making charcoal from biomass. *Combustion:* Process of burning in air. *Ignition:* the act of starting combustion. *Exothermic.* Releases heat. *Ignitable:* can catch on fire. *Seal:* to close so no air can enter or exit. *Inert atmosphere:* environment that doesn't have oxygen so that carbonization can take place.

**INSTRUCTIONS.** Each row equals a stage of the charcoal burn. Each column signifies a burn. For stages 1 and 9, the mass of initial and final material needs to be recorded in kg, g, or other units (must use the same units for both). For stages 2 to 8, the time at which each stage starts needs to be recorded. Once the burn is done, you can calculate the char yield using the formula in row 10 and record it. There is space for recording 10 burns in 10 columns. For each burn, record the conditions in the table below. By comparing char yields, you can find which conditions result in better yields. Some examples of conditions you can change are: material, use corncobs only; packing density: using more or less material in the same sized kiln; seal time. Changing only one parameter per burn will make it easier to know exactly which condition caused change. You can repeat the same burn to confirm the results.

#	DAY	OPERATOR	MATERIAL	DRYING TIME	COMMENTS
0	28 dec 2015	Dan Sweeney	Corn cobs	18 days	The burn took longer than usual to finish.
1					
2					
3					
4					
5					
6					
7					
8					
9					
10					

Figure 4-2: Charcoal burn worksheet Page 2.



# Chapter 5

## Conclusion

Studies of the pyrolysis of three types of corn-based feedstock: cobs, husks, and stalks were successfully performed using TGA-MS techniques. The mass loss data obtained was used for the calculation of proximate analysis in terms of moisture, volatile matter and char content. TG-DTG data provided insight about the impact that the different ligno-cellulosic composition of the three materials had in the pyrolysis reactions occurring between 200 °C and 500 °C. Corn cobs showed to be best suited feedstocks for charcoal production due to their higher char content and lower moisture content. Mass Spectroscopy relative abundance data as a function of the temperature profile proved useful to analyze emissions of water, carbon monoxide, hydrogen sulfide and aromatic compounds, and provided information about the unexpected mass loss occurring between 800 °C and 900 °C, which likely corresponds to the oxidation of carbon. The kinetic data obtained for  $E_a$  and  $A$  for cobs and husks using the first order single global reaction model matched that of literature, and supported the use of cobs as feedstock. Further work is needed to obtain mass loss data for more heating rates, which could lead to more reliable  $E_a$  and  $A$  calculations, and could also be used in other models. The first draft of a worksheet to facilitate monitoring of char yield with varying carbonization conditions in the field was created and is waiting for implementation and improvement.



# Appendix A

## MATLAB Code

### A.1 TGA-DTGA Data Analysis

```
1 format long;
2 alldata = csvread('cc-n2-foran.csv'); %import data
3 time = alldata(:,1); % time vector in min
4 temp = alldata(:,2); % temperature vector in C
5 mass = alldata(:,3); % mass vector in mg
6 weiper = alldata(:,4); % mass percentage vector in %
7 dWdT_0 = alldata(:,5); % DTG wrt temperature vector created by Trios software
8 dWdT_1 = abs(dWdT_0); % DTG is now positive
9 dWdT = (1-0)./(max(dWdT_1)-min(dWdT_1))* %moved below to fit page
10 ((dWdT_1-max(dWdT_1))+max(dWdT_1)); %Normalize derivative to 1
11 %Find Ti = pyrolysis initial temperature and its location
12 der_ran = find(dWdT>0.03 & dWdT<0.031); %Set derivative sensitivity
13 Ti_temps = temp(der_ran);
14 TP_ix_loc = find(Ti_temps>150 & Ti_temps<250,1);
15 P_Ti = Ti_temps(TP_ix_loc);
16 P_Ti_loc = find(temp>P_Ti,1);
17 %Find Tf = pyrolysis final temperature and its location
18 TP_fx_loc = find(Ti_temps>300,1);
19 P_Tf = Ti_temps(TP_fx_loc);
```

```

20 P_Tf_loc = find(temp>P_Tf,1);
21 max_mass = max(mass);
22 %Calculate M = moisture percentage
23 M_mloss = mass(1) - mass(P_Ti_loc);
24 M = M_mloss/max_mass*100;
25 %Calculate VM = volatile matter percentage
26 VM_mloss = mass(P_Ti_loc) - mass(P_Tf_loc);
27 VM = VM_mloss/max_mass*100;
28 %Calculate C = charcoal percentage
29 C = mass(end)/max_mass*100;

```

## A.2 $E_a$ calculation

```

1 % Import data from text file
2 alldata_h2 = csvread('ch-5h-2c-foran.csv');
3 heat_rate_h2 = 2/60; %in C/s
4 temp_h2_0 = alldata_h2(:,2);
5 temp_h2 = temp_h2_0+273.15; %in K
6 weiper_h2 = alldata_h2(:,4);
7 dWdT_h2_0i = alldata_h2(:,5);
8 dWdT_h2_0 = abs(dWdT_h2_0i);
9 dWdT_h2 = (1-0)./(max(dWdT_h2_0)-min(dWdT_h2_0))* %moved below to fit page
10 ((dWdT_h2_0-max(dWdT_h2_0))+max(dWdT_h2_0));
11 alldata_h3 = csvread('ch-2h-10c-foran.csv');
12 heat_rate_h3 = 10/60; %in C/s
13 temp_h3_0 = alldata_h3(:,2);
14 temp_h3 = temp_h3_0+273.15; %in K
15 weiper_h3 = alldata_h3(:,4);
16 dWdT_h3_0i = alldata_h3(:,5);
17 dWdT_h3_0 = abs(dWdT_h3_0i);
18 dWdT_h3 = (1-0)./(max(dWdT_h3_0)-min(dWdT_h3_0))*
19 ((dWdT_h3_0-max(dWdT_h3_0))+max(dWdT_h3_0)); %moved below to fit page
20 %Find mass loss equivalences
21 %-20% mass loss

```



```

22 h2_20_r = find(weiper_h2>80 & weiper_h2<80.01);
23 h2_20 = temp_h2(h2_20_r);
24 h3_20_r = find(weiper_h3>80 & weiper_h3<80.05);
25 h3_20 = temp_h3(h3_20_r);
26 %-30% mass loss
27 h2_30_r = find(weiper_h2>70 & weiper_h2<70.01);
28 h2_30 = temp_h2(h2_30_r);
29 h3_30_r = find(weiper_h3>70 & weiper_h3<70.05);
30 h3_30 = temp_h3(h3_30_r);
31 %-40% mass loss
32 h2_40_r = find(weiper_h2>60 & weiper_h2<60.01);
33 h2_40 = temp_h2(h2_40_r);
34 h3_40_r = find(weiper_h3>60 & weiper_h3<60.05);
35 h3_40 = temp_h3(h3_40_r);
36 %-50% mass loss
37 h2_50_r = find(weiper_h2>50 & weiper_h2<50.02);
38 h2_50 = temp_h2(h2_50_r);
39 h3_50_r = find(weiper_h3>50 & weiper_h3<50.1);
40 h3_50 = temp_h3(h3_50_r);
41 %-60% mass loss
42 h2_60_r = find(weiper_h2>40 & weiper_h2<40.01);
43 h2_60 = temp_h2(h2_60_r);
44 h3_60_r = find(weiper_h3>40 & weiper_h3<40.05);
45 h3_60 = temp_h3(h3_60_r);
46 %Find Ea = slope for each mass loss
47 x1_0 = [h2_20 h3_20];
48 y1_0 = [heat_rate_h2 heat_rate_h3]
49 x1 = 1./x1_0;
50 y1 = -log(y1_0);
51 x2_0 = [h2_30 h3_30];
52 y2_0 = [heat_rate_h2 heat_rate_h3]
53 x2 = 1./x2_0;
54 y2 = -log(y2_0);
55 x3_0 = [h2_40 h3_40];
56 y3_0 = [heat_rate_h2 heat_rate_h3]
57 x3 = 1./x3_0;

```

```

58 y3 = -log(y3_0);
59 x4_0 = [h2_50 h3_50];
60 y4_0 = [heat_rate_h2 heat_rate_h3]
61 x4 = 1./x4_0;
62 y4 = -log(y4_0);
63 x5_0 = [h2_60 h3_60];
64 y5_0 = [heat_rate_h2 heat_rate_h3]
65 x5 = 1./x5_0;
66 y5 = -log(y5_0);
67 coef1 = polyfit(x1,y1,1);
68 slope1 = coef1(1);
69 Ea(1) = slope1 * -8.3145/2.18923;
70 coef2 = polyfit(x2,y2,1);
71 slope2= coef2(1);
72 Ea(2) = slope2 * -8.3145/2.18923;
73 coef3 = polyfit(x3,y3,1);
74 slope3 = coef3(1);
75 Ea(3) = slope3 * -8.3145/2.18923;
76 coef4 = polyfit(x4,y4,1);
77 slope4 = coef4(1);
78 Ea(4) = slope4 * -8.3145/2.18923;
79 coef5 = polyfit(x5,y5,1);
80 slope5 = coef5(1);
81 Ea(5) = slope5 * -8.3145/2.18923;
82 %Calculate E_a
83 Ea_avg = mean(Ea)/1000; %in KJ/mol

```

### A.3 A calculation

```

1 format long;
2 %%2 C/min Heating rate = h2
3 %import data
4 alldata_h2 = csvread('cc-5h-2c-foran.csv');
5 heat_rate_h2 = 2/60; %in deg/s

```

```

6 temp_h2_0 = alldata_h2(:,2);
7 temp_h2 = temp_h2_0+273.15; %in K
8 mass_h2 = alldata_h2(:,3); %alfa is unitless so units dont matter
9 weiper_h2 = alldata_h2(:,4);
10 %initial mass at -20% loss
11 h2_20_loc = find(weiper_h2>80 & weiper_h2<80.01);
12 h2_mi = mass_h2(h2_20_loc);
13 %final mass at -60% loss
14 h2_60_loc = find(weiper_h2>40 & weiper_h2<40.01);
15 h2_mf = mass_h2(h2_60_loc);
16 %Find temperatures and masses for -30%, -40% and -50%
17 h2_30_loc = find(weiper_h2>70 & weiper_h2<70.01);
18 h2_30_T = temp_h2(h2_30_loc);
19 h2m_30 = mass_h2(h2_30_loc);
20 h2_40_loc = find(weiper_h2>60 & weiper_h2<60.01);
21 h2_40_T = temp_h2(h2_40_loc);
22 h2m_40 = mass_h2(h2_40_loc);
23 h2_50_loc = find(weiper_h2>50 & weiper_h2<50.02);
24 h2_50_T = temp_h2(h2_50_loc);
25 h2m_50 = mass_h2(h2_50_loc);
26 %get alfas and g(x)
27 alfa30_h2 = (h2_mi - h2m_30)/(h2_mi-h2_mf);
28 g_alfa30_h2 = -log(1-alfa30_h2);
29 alfa40_h2 = (h2_mi - h2m_40)/(h2_mi-h2_mf);
30 g_alfa40_h2 = -log(1-alfa40_h2);
31 alfa50_h2 = (h2_mi - h2m_50)/(h2_mi-h2_mf);
32 g_alfa50_h2 = -log(1-alfa50_h2);
33 %p(x) tabulated from E and T by Zsako 1968
34 p30_h2 = 10.544;
35 p40_h2 = 10.401;
36 p50_h2 = 10.126;
37 %calculate B = the pre-exponential factor
38 B_h2(1) = log10(g_alfa30_h2) + p30_h2;
39 B_h2(2) = log10(g_alfa40_h2) + p40_h2;
40 B_h2(3) = log10(g_alfa50_h2) + p50_h2;
41 B2 = mean(B_h2);

```



# Bibliography

Aboyade, A.O., Hugo, T.J., Carrier, M., Meyer, E.L., Stahl, R., Knoetze, J.H., Gorgens, J.F. (2011). Non-isothermal kinetic analysis of the devolatilization of corn cobs and sugar cane bagasse in an inert atmosphere. *Thermochimica Acta*, 57(1—2) 81—89.

Barten, T. J. (2013). Evaluation and prediction of corn stover biomass and composition from commercially available corn hybrids by. Iowa State University.

Basu, P. (2013). Biomass gasification, pyrolysis, and torrefaction: practical design and theory, second edition. San Diego, CA: Academic Press, 2013.

Bogale, W. (2009). Preparation of Charcoal Using Agricultural Wastes. *Ethiopian Journal of Education and Science*, 5(1), 79—93.

Bridgeman, T.G., Darvell, L.I., Jones, J.M., Williams, P.T., Fahmi, R., Bridgewater, A.V., Barraclough, T., Shield, I., Yates, N., Thain, S.C., Donnison, I.S. (2007) Influence of particle size on the analytical and chemical properties of two energy crops. *Fuel* 86(1—2), 60—72.

Broadhead, J., Bahdon, J., & Whiteman, A. (2001). Past trends and future prospects for the utilisation of wood for energy. *Global Forest Products Outlook Study Working Paper*, (5).

Demirbas, A. (1999). Properties of charcoal derived from hazelnut shell and the production of briquettes using pyrolytic oil, 24, 141—150.

Demirbas, A. (2001). Biomass resource facilities and biomass conversion processing for fuels and chemicals. *Energy Conversion and Management*, 42(11), 1357—1378.

Emrich, W. (1985). *Handbook of charcoal making: the traditional and industrial methods*.

*Encyclopedia Americana*. (1994).

Flynn, J. H., & Wall, L. A. (1966). A quick, direct method for the determination of activation energy from thermogravimetric data. *Polymer Letters*, 4(1), 323-328.

United States Environmental Protection Agency. (2005). *Climate Leaders Greenhouse Gas Inventory Protocol: Design Principles*.

Fuel from the Fields Charcoal Do It. (n.d.). MIT D-Lab. Cambridge, MA.

Gabott, P. (Ed.). (2008). *Applications of Thermal Analysis* (1st ed.). Blackwell Publishing Ltd.

Griscom, B., Ganz, D., Virgilio, N., Price, F., Hayward, J., Cortez, R., Stanley, B. (2009). *The Hidden Frontier of Forest Degradation: A Review of the Science, Policy and Practice of Reducing Degradation Emissions*. Arlington, VA.

Haykiri-Acma, S. Yaman, S. Kucukbayrak (2006). Effect of heating rate on the pyrolysis yields of rapeseed. *Renewable Energy*, 31 (2006), 803—810.

International Energy Agency. *Energy for Cooking in Developing Countries*. (2006). Chapter 9, In *World Energy Outlook* (pp. 419—445).

J-Pal Policy Briefcase. (2012). *Up in smoke*. Cambridge, MA.

Koppmann, R., Czapiewski, K. Von, & Reid, J. S. (2005). A review of biomass burning emissions, part I: gaseous emissions of carbon monoxide, methane. *Atmospheric Chemistry and Physics Discussions*, European Geosciences Union, 5(5), 10455—10516.

Lanzetta, M & Di Blasi, C. (1998). Pyrolysis kinetics of wheat and corn straw. *Journal of Analytical and Applied Pyrolysis*. 44(2), 181—192.

Lee, D., Owens, V. N., Boe, A., & Jeranyama, P. (2007). *Composition of Herbaceous Biomass Feedstocks*. Sun Grant Initiative, North Central Center, South Dakote State University. Brookings, SD.

Li, Z., Zhao, W., Meng, B., Liu, C., Zhu, G., Zhao, G. (2008). Kinetic study of corn straw pyrolysis: Comparison of two different three-pseudocomponent models. *Bioresource Technology*, 99(16), 7616—7622.

Liu, Z., Qin, L., Li, B., & Yuan, Y. (2015). Physical and Chemical Characterizations of Corn Stover from Leading Pretreatment Methods and Effects on Enzymatic Hydrolysis. *ACS Sustainable Chemistry & Engineering*, 3(1), 140—146.

Mani, T., Murugan, P., Abedi, J., Mahinpey, N. Pyrolysis of what straw in thermogravimetric analyzer: Effect of particle size and heating rate on devolatilization and estimation of global kinetics. (2010). *Chemical Engineering Research and Design*, 88(8), 952—958.

Mendoza, R. U. (2011). Why do the poor pay more? Exploring the poverty penalty concept, 28(1), 1—28.

Olivier, J. G. J., Janssens-Maenhout, G., Peters, J. A. H. W., & Wilson, J. (2011). Long-term trends in global CO<sub>2</sub> emissions. PBL Netherlands Environmental Assessment Agency.

Parikh, J, Channiwala, S.A & Ghosal, G.K. (2007) A correlation for calculating elemental composition from proximate analysis of biomass materials, *Fuel*. 86(12—13), 1710—1719.

Protasio, T. D. P., Trugilho, P. F., Mirmehdi, S., & Gomes, M. (2014). Quality and Energetic Evaluation of the Charcoal Made of Babassu Nut Residues in the Steel Industry. *Cienc. Agrotec.*, 38(5), 435—444.

Putti, V. R., Tsan, M., Mehta, S., & Kammila, S. (2015). The state of the global clean and improved cooking sector. Washington DC, USA.

Quartey, E. B. O. T. (2008). Briquetting agricultural waste as an energy source in Ghana. *Recent Researches in Environment, Energy Planning and Pollution*, 200—204.

Schure, J. (2012). 5. Woodfuel and producers'livelihoods in the Congo Basin. Centre for International Forestry Research (CIFOR), Wageningen University, Forest and Nature Conservation Policy Group (FNP).

Singh, M., Stanley, R., Vechakul, J., Smith, A., Banzaert, A., & Frayne, S. (2010). *Fuel from the Fields: Charcoal from Agricultural Waste*. Warwickshire, UK.

Sinha, S., Jhalani, A., Ravi, M. R., & Ray, A. (n.d.). Modelling of Pyrolysis in Wood: A Review. *SESI Journal*, 10(1): 41-62.

Stamm, A. J. (1956). Thermal Degradation of Wood and Cellulose. *Industrial & Engineering Chemistry*, 48(3), 413—417.

Tiwari, P., & Deo, M. (2012). Compositional and kinetic analysis of oil shale pyrolysis using TGA—MS. *Fuel*, 94, 333—341.

World Health Organization. *Fuel for Life Household Energy and Health*. (2006). Geneva, Switzerland.

World Health Organization. WHO guidelines for indoor air quality: household fuel combustion. (2014). Geneva, Switzerland.

World Bank. (2011). Wood-Based Biomass Energy Development for Sub-Saharan Africa. Africa Renewable Energy Access Program.

Yang, H., Yan, R., Chen, H., Zheng, C., Lee, D. H., Uni, V. (2006). In-Depth Investigation of Biomass Pyrolysis Based on Three Major Components: Hemicellulose, Cellulose and Lignin. *ACS Energy Fuels*, 20(1), 388—393.

Zabaniotou, A., Ioannidou, O. (2008). Evaluation of utilization of corn stalks for energy and carbon material production by using rapid pyrolysis at high temperature. *Fuel*, 87(6), 834-843.

Zsako, J., & Zsako, J. J. (1980). Kinetic Analysis of Thermogravimetric Data XIV. Three Integral Methods and Their Computer Programs. *Journal of Thermal Analysis*, 19, 333—345.